

# Characterization of entanglement of more than two qubits with Bell inequalities and global entanglement

Jochen Endrejat\* and Helmut Büttner

*Theoretische Physik I, Universität Bayreuth, D-95440 Bayreuth, Germany*

(Dated: November 15, 2018)

It is shown that the entanglement-structure of 3- and 4-qubit states can be characterized by optimized operators of the Mermin-Klyshko type. It is possible to discriminate between pure 2-qubit entanglements and higher entanglements. A comparison with a global entanglement measure and the i-concurrence is made.

PACS numbers: 03.67.Mn, 03.65.Ud, 75.10.Jm

## I. INTRODUCTION

There seems to be no doubt in the literature that entanglement of quantum mechanical states is one of the important ingredients in the broad field of quantum information theory. Many protocols in this area are based on entangled states, it is the basis of quantum cryptography [1], super dense coding [2], teleportation [3] and other fields. Although it is an important ingredient entanglement is even called puzzling, and especially genuine multipartite entanglement for 3- and 4-qubits is a field of active research, because only for two qubits a correct measure for their entanglement is available.

In this paper we will give a new method of characterization of 3- and 4-qubit entanglement.

In the following we will show how different measures for quantifying entanglement can be applied to a model spin system which can be used as a basis for many different experimental setups. It is a one-dimensional Heisenberg spin system with different arrangements for 3- and 4 spins. We will compare a global entanglement measure [4] with the results of Bell inequalities in the form proposed by Mermin and Klyshko [5, 6, 7] which means that we look for a measure with optimized polynomial spin operators. It will be shown that the optimized polynomials measure the different degrees of entanglement astonishing well.

The paper is structured as follows: In chapter II a special form of Bell inequalities is described for 3- and 4-qubit systems. We also define a new method how to handle these polynomial inequalities. In chapter III we shortly discuss the global entanglement measure and describe its relation to concurrences as well as to 3-qubit tangle measure. In chapter IV these measures are applied to the general Greenberger Horne Zeilinger (GHZ) state for 3-qubits and the surprising result is that the optimized Mermin-Klyshko operators are well suited to describe the entanglement as well as the global entanglement over a wide range of parameters. In chapter V we now apply these different measures to the special form of a 3-qubit

Heisenberg spin system and again it turned out that for the pure eigenstates and for the superposition of these eigenstates the optimized Bell operator as well as the global entanglement measure are in excellent agreement describing the entanglement. In chapter VI we have a look at a 4-qubit system and compare it with the 3-qubit results. A discussion follows in the concluding chapter VII.

## II. SPIN-POLYNOMIALS FOR ENTANGLEMENT MEASURE

From Bell-Inequalities various polynomials are known for entanglement-classifications. We use here the Mermin-Klyshko polynomials which were discussed by Yu et al. [8] in their classification scheme. We propose a special optimization procedure to give a quantitative analyse of Heisenberg spin models.

We test our method for 3-qubit systems and then apply it to 4-qubits, where it is shown that the resulting optimized Mermin-Klyshko operators are able to quantitatively describe the total entanglement measures. Furthermore, comparing it with the sum of the 2-qubit concurrences the difference gives a measure to the additional 3- and 4-qubit entanglements. We note already here that the optimization procedure yields many equivalent minima, therefore it is not possible to extract directly a single well defined operator polynomial.

### A. 3 qubits

For 3-qubits the polynomials can be written as products of spin operators [8]:

$$F_3 = (AB' + A'B)C + (AB - A'B')C' \quad (1)$$

$$F'_3 = (AB' + A'B)C' - (AB - A'B')C \quad (2)$$

where the operators are written as sums of Pauli matrices.

$$A^{(\prime)} = \vec{a}^{(\prime)} \cdot \vec{\sigma}_A, \quad B^{(\prime)} = \vec{b}^{(\prime)} \cdot \vec{\sigma}_B, \quad C^{(\prime)} = \vec{c}^{(\prime)} \cdot \vec{\sigma}_C$$

with  $\vec{a}^{(\prime)}$ ,  $\vec{b}^{(\prime)}$  and  $\vec{c}^{(\prime)}$  normalised vectors and the Pauli matrices  $\vec{\sigma}_A$ ,  $\vec{\sigma}_B$ ,  $\vec{\sigma}_C$ , referring to the qubits  $A$ ,  $B$  and  $C$ ,

\*Electronic address: jochen.endrejat@uni-bayreuth.de

with  $\vec{\sigma}_i = (\sigma_i^x, \sigma_i^y, \sigma_i^z)$ .

The classification for pure 3-qubit states is as follows. (For details we refer to [8].) We look for the maximum of the absolute values of the expectation values of these polynomials and find for pure product states:

$$\max\{|\langle F_3 \rangle_\rho|, |\langle F'_3 \rangle_\rho|\} \leq 2 \quad (3)$$

The other inequalities found in [8] can be written as

$$\langle F_3 \rangle_\rho^2 + \langle F'_3 \rangle_\rho^2 \leq 2^3 \quad (4)$$

if the state is 2-qubit entangled and

$$\langle F_3 \rangle_\rho^2 + \langle F'_3 \rangle_\rho^2 \leq 2^4 \quad (5)$$

if the state is 3-qubit entangled.

Our method consists in a numerical optimization of the components of the vectors  $\vec{a}^{(l)}$ ,  $\vec{b}^{(l)}$  and  $\vec{c}^{(l)}$  of these polynomials. We used the NAG library function e04ucc [19] with randomly chosen initial conditions.

Since it was not clear from [8] we applied two different methods. In the first approach we look for the expectation value of  $F_3$  and maximize it. The polynomial  $F'_3$  is calculated with these parameters and then the sum  $\langle F_3 \rangle_\rho^2 + \langle F'_3 \rangle_\rho^2$  is determined.

In the second approach we directly maximized the sum of the squares since all these inequalities are sufficient but not necessary. By comparing the results of the optimization with each other and with other measures of entanglement we found that the first described method, the optimization of the  $F_3$ -operator yields the best information.

Since we have not seen this numerical investigation even for the simplest states used in the literature we cite the following results, obtained with the first described method.

For the GHZ-state [9]  $(|000\rangle + |111\rangle)/\sqrt{2}$ :

$$\begin{aligned} \max\{|\langle F_3 \rangle_{GHZ}|\} &= 4.00 \\ \Rightarrow |\langle F'_3 \rangle_{GHZ}| &= 0; \quad \langle F_3 \rangle_{GHZ}^2 + \langle F'_3 \rangle_{GHZ}^2 = 16.00 \end{aligned}$$

while for the so-called W-state [10]  $(|001\rangle + |010\rangle + |100\rangle)/\sqrt{3}$  we can list the following results which show that there seems to be a 3-party entanglement although compared to GHZ it has not the maximum possible value.

$$\begin{aligned} \max\{|\langle F_3 \rangle_W|\} &= 3.05 \\ \Rightarrow |\langle F'_3 \rangle_W| &= 0.05 \quad \langle F_3 \rangle_W^2 + \langle F'_3 \rangle_W^2 = 9.305 \end{aligned}$$

### B. 4 qubits

The sufficient conditions for 4-qubits are a little more involved since we have to introduce an additional spin polynomial for the 4<sup>th</sup> qubit but we can write altogether

$$F_4 = \frac{1}{2}(D + D') \otimes F_3 + \frac{1}{2}(D - D') \otimes F'_3 \quad (6)$$

$$F'_4 = \frac{1}{2}(D + D') \otimes F'_3 + \frac{1}{2}(D' - D) \otimes F_3, \quad (7)$$

where  $F_3$  and  $F'_3$  are defined in (1) resp. (2) and  $D^{(l)} = \vec{a}^{(l)} \cdot \vec{\sigma}_D$  are the spin operators on the 4<sup>th</sup> qubit  $D$ . The classification scheme after Yu et al. [8] is as follows. Product states fulfil the following inequality:

$$\max\{|\langle F_4 \rangle_\rho|, |\langle F'_4 \rangle_\rho|\} \leq 2 \quad (8)$$

And for distinguishing different kinds of entanglement one can use the following scheme which gives sufficient but not necessary classification.

- 2-qubit entanglement:  $\langle F_4 \rangle_\rho^2 + \langle F'_4 \rangle_\rho^2 \leq 8$
- 3-qubit entanglement:  $\langle F_4 \rangle_\rho^2 + \langle F'_4 \rangle_\rho^2 \leq 16$
- 4-qubit entanglement:  $\langle F_4 \rangle_\rho^2 + \langle F'_4 \rangle_\rho^2 \leq 32$ ,

where the description [8] is as follows. 4-qubit entanglement means a state with fully entangled 4-qubits, 3-qubit entanglement describes a product-state of one qubit with fully entangled 3-qubits, and 2-qubit entanglement can be a product of two 2-qubit entangled states or a 2-qubit entangled state as product with two single qubits. Before applying these inequalities to the spin-systems we discuss another useful measure.

### III. I-CONCURRENCES AND GLOBAL ENTANGLEMENT

The original measure  $Q$  of a many qubit pure state  $|\psi\rangle$  was introduced by Meyer and Wallach [4]. It was later shown by Brennen [11] that this kind of global entanglement can be written as

$$Q(|\psi\rangle) = 2[1 - 1/n \sum_{k=1}^n Tr(\rho_k^2)], \quad (9)$$

with  $\rho_k$ , the density matrix reduced to a single qubit  $k$ . It is interesting to note that there can be introduced the so-called i-concurrence [12] which also is directly related to the reduced density matrix  $\rho_A$  of a subsystem  $A$ . This i-concurrence measures the entanglement between two subsystems  $A$  and  $B$  and can be written as

$$IC_{A-B} = \sqrt{2[1 - Tr(\rho_A^2)]} \quad (10)$$

In the following we use the notation  $IC_{A-B} \equiv IC_A$ . We find as first result that the global entanglement  $Q$  is directly related to the sum of the squares of the i-concurrences of the 1-qubit subsystems of a  $N$  qubit state

$$Q = 1/N \sum_{i=1}^N IC_i^2 \quad (11)$$

### A. 3 qubits

For the special case of 3-qubits one can introduce the so-called tangle  $\tau_{123}$  [13] which in a sense describes those contributions to the i-concurrences which are not described by 2-qubit concurrences [14, 15]

$$IC_1^2 = C_{12}^2 + C_{13}^2 + \tau_{123} \quad (12)$$

$$IC_2^2 = C_{12}^2 + C_{23}^2 + \tau_{123} \quad (13)$$

$$IC_3^2 = C_{13}^2 + C_{23}^2 + \tau_{123} \quad (14)$$

We can sum these relations up

$$\sum_{i=1}^3 IC_i^2 = 2(C_{12}^2 + C_{13}^2 + C_{23}^2) + 3\tau_{123} \quad (15)$$

and introduce this into the global entanglement. It is nicely seen that for 3 qubits this consists of the sum of squared 2-qubit concurrences plus the additional tangle:

$$Q = \frac{2}{3}(C_{12}^2 + C_{13}^2 + C_{23}^2) + \tau_{123} \quad (16)$$

The total entanglement measure is the sum of different entanglement contributions.

### B. 4 qubits

These nice results for 3-qubits cannot easily be extended to 4-qubits since there is no equivalent definition of the corresponding higher tangle. But to give an impression of the power of the description with a global measure one can look for special qubit states where there are effectively only 2-qubit concurrences.

$$|\phi\rangle = \alpha_1|1000\rangle + \alpha_2|0100\rangle + \alpha_3|0010\rangle + \alpha_4|0001\rangle \quad (17)$$

One easily finds that the i-concurrences are sums of 2-qubits concurrences and therefore the global entanglement can be written as

$$Q = \frac{1}{2}(C_{12}^2 + C_{13}^2 + C_{14}^2 + C_{23}^2 + C_{24}^2 + C_{34}^2). \quad (18)$$

Again this indicates a good total measure of entanglement by the value of  $Q$ .

## IV. APPLICATION TO GENERALIZED GHZ-STATE

One result of our investigations is that the comparison of sufficient conditions from the Bell inequalities and the global expression  $Q$  is an appropriate measure for the entanglement of 3- and 4-qubits.

As a first test we consider the generalised GHZ state for 3 qubits written as

$$g|000\rangle + \sqrt{1-g^2}|111\rangle, \quad (19)$$

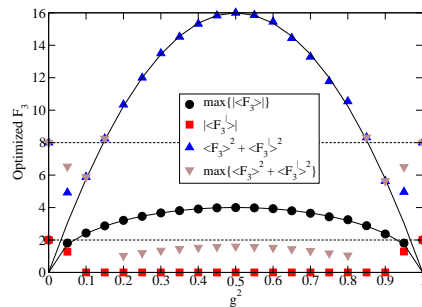


FIG. 1: Optimization of the expectation value of  $F_3$  for the 3-qubit generalized GHZ-state as a function of  $g^2$ ; the course of  $\max\{|\langle F_3 \rangle|\}$  is fitted with  $y = c_0 g \sqrt{1-g^2}$ , with  $c_0 = 8.01$ ; the course of  $\langle F_3 \rangle^2 + \langle F_3' \rangle^2$  with  $y = c_1 g^2 (1-g^2)$  and  $c_1 = 64.01$ ;  $\max\{\langle F_3 \rangle^2 + \langle F_3' \rangle^2\}$  marks the optimization of the squared inequalities. The dashed lines mark the boundaries arising from the inequalities (3) resp. (4). See text for more discussion.

with  $g \in [0, 1]$ . It is well known that there are no 2-qubit concurrences so that the remaining i-concurrences

$$IC_1 = IC_2 = IC_3 = 2g\sqrt{1-g^2} \quad (20)$$

mainly measure the tangle of the state which is of course parameter dependent and from our formula (16) it can be seen that  $Q$  just measures this tangle:

$$Q = \tau_{123} = 4g^2(1-g^2) \quad (21)$$

In fig. 1 the results of the Bell optimization are plotted as a function of  $g^2$ .  $\max\{|\langle F_3 \rangle|\}$  means the optimization of the expectation value of  $F_3$ . Then the resulting parameters are introduced in the expectation value of  $F_3'$  (Notation:  $|\langle F_3' \rangle|$ ) and the squared inequalities (4) respectively (5) (Notation:  $\langle F_3 \rangle^2 + \langle F_3' \rangle^2$ ). This procedure yields results that are nearly identical to the parameter dependence of the i-concurrence and the tangle resp.  $Q$  (cp. (21)) over a large parameter range. This fact is underlined with the fit of the results of the inequalities by the results of the i-concurrences resp. the tangle. We therefore conclude that our maximization procedure yields the correct information for the entanglement. (Note however that the optimization procedure as with all search-algorithms may fail to find the appropriate maximum.) Only for a small parameter range ( $0 < g < 0.39$  and  $0.92 < g < 1$ ) the inequalities are not sufficient compared to the calculated tangle. These results show that at the boundaries of the parameter values the optimization of  $F_3$  could have problems but over a large range of the parameter values the optimized  $F_3$  gives a good measure of entanglement as the tangle itself although we have no direct proof of the equivalence of these two measures. Quite remarkable is here the fact that the optimization of  $\langle F_3 \rangle^2 + \langle F_3' \rangle^2$  (Notation:  $\max\{\langle F_3 \rangle^2 + \langle F_3' \rangle^2\}$ ) yields for the parameter values  $0.39 < g < 0.92$  no sufficient criterion for entanglement.

The points ( $g = 0.26$  and  $g = 0.97$ ) where the inequality (3) is not violated agree with the results derived by

Scarani and Gisin [16].

This successful description of the generalized GHZ-states encourages us to describe the entanglement of more complex systems.

## V. PURE 3-QUBIT HEISENBERG STATES

As in reference [17] already discussed, Heisenberg spin systems are good models for various experimental realizations of multi-qubit systems. Here we look for a special chain of 3 qubits where the interaction between qubit 1 and 2 and 2 and 3 are given by a certain interaction constant while between 1 and 3 we have doubled the interaction. Our main purpose is, however, to study the anisotropy effect of this Hamiltonian given by

$$H = \frac{J}{4} \left( \sigma_1^x \sigma_2^x + \sigma_1^y \sigma_2^y + \Delta \sigma_1^z \sigma_2^z + \sigma_2^x \sigma_3^x + \sigma_2^y \sigma_3^y + \Delta \sigma_2^z \sigma_3^z \right) + \frac{J}{2} \left( \sigma_1^x \sigma_3^x + \sigma_1^y \sigma_3^y + \Delta \sigma_1^z \sigma_3^z \right), \quad (22)$$

with the anisotropy coefficient  $\Delta$ . The eigensystem of this Hamiltonian is calculated in the computational basis. The eigenvalues and eigenstates are given in Table I.

The eigenstates are of course partially degenerated because of the spin symmetry of the system. This can be easily lifted by an applied field

$$H' = H + \frac{M}{2} \sum_{i=1}^3 \sigma_i^z, \quad (23)$$

so that in the following we think of the different eigenstates as pure states and discuss only the parameter dependent eigenstates  $|\psi_5\rangle$  to  $|\psi_8\rangle$  because we are interested in the change of entanglement with different anisotropy strengths. Since the 2-qubit measures are known we will get more insight into pure 3-qubit entanglement. As it

TABLE I: Eigensystem of the 3-qubit Hamiltonian

$E_1 = \Delta J$	$ \psi_1\rangle =  111\rangle$
$E_2 = \Delta J$	$ \psi_2\rangle =  000\rangle$
$E_3 = -\frac{J}{2}$	$ \psi_3\rangle = -\frac{1}{\sqrt{2}}( 011\rangle -  110\rangle)$
$E_4 = -\frac{J}{2}$	$ \psi_4\rangle = -\frac{1}{\sqrt{2}}( 001\rangle -  100\rangle)$
$E_5 = -\frac{J}{4}(\eta + \Delta - 2)$	$ \psi_5\rangle = \frac{\sqrt{\chi}}{2\sqrt{\eta}} \left(  011\rangle - \frac{4}{\chi} 101\rangle +  110\rangle \right)$
$E_6 = -\frac{J}{4}(\eta + \Delta - 2)$	$ \psi_6\rangle = \frac{\sqrt{\chi}}{2\sqrt{\eta}} \left(  100\rangle - \frac{4}{\chi} 010\rangle +  001\rangle \right)$
$E_7 = \frac{J}{4}(\eta - \Delta + 2)$	$ \psi_7\rangle = \frac{\sqrt{2}}{\sqrt{\eta}\sqrt{\chi}} \left(  011\rangle + \frac{\chi}{2} 101\rangle +  110\rangle \right)$
$E_8 = \frac{J}{4}(\eta - \Delta + 2)$	$ \psi_8\rangle = \frac{\sqrt{2}}{\sqrt{\eta}\sqrt{\chi}} \left(  100\rangle + \frac{\chi}{2} 010\rangle +  001\rangle \right)$

with:

$$\eta = \sqrt{12 + \Delta(\Delta - 4)} \quad \text{and} \quad \chi = \eta + \Delta - 2$$

was seen for the generalized GHZ-state the parameter dependence of the states gives insight into the effectiveness of different entanglement measures.

### A. The states $|\psi_5\rangle, |\psi_6\rangle$

We start with the states  $|\psi_5\rangle$  and  $|\psi_6\rangle$  which yield the same results in measuring the entanglement. The concurrences are calculated to be:

$$C_{12} = C_{23} = \frac{2}{\eta} \quad C_{13} = \frac{4}{\eta^2 - (\Delta - 2)\eta}. \quad (24)$$

In the limit  $\Delta \rightarrow \infty$  the states have an easy form

$$|\psi_5\rangle \approx \frac{1}{\sqrt{2}}(|01\rangle_{13} + |10\rangle_{13}) \otimes |1\rangle_2$$

$$|\psi_6\rangle \approx \frac{1}{\sqrt{2}}(|01\rangle_{13} + |10\rangle_{13}) \otimes |0\rangle_2$$

and the results for the concurrences are consistent with this form.  $C_{12}$  and  $C_{23}$  are vanishing while  $C_{13}$  increases to one. The sum of the squared concurrences is needed for calculating  $Q$

$$\sum C_{ij}^2 = 8 \left( \frac{1}{\eta^2} + \frac{2}{(\eta^2 - (\Delta - 2)\eta)^2} \right) \quad (25)$$

To calculate the tangle  $\tau_{123}$  one needs the i-concurrences

$$IC_1 = IC_3 = \frac{1}{\sqrt{2}} \sqrt{1 + \frac{4}{\eta^2} + \frac{\Delta - 2}{\eta}} \quad (26)$$

$$IC_2 = \frac{2\sqrt{2}}{\eta} \quad (27)$$

From these equations and the results for the concurrence it follows with (12) that  $\tau_{123} = 0$ . Therefore the total global entanglement  $Q$  is given mainly by the squares of the concurrences as it follows from equation (16), and its parameter dependence is shown in fig. 2.

### B. The states $|\psi_7\rangle, |\psi_8\rangle$

The states  $|\psi_7\rangle$  and  $|\psi_8\rangle$  have the same results for entanglement measurement as well. The concurrences are calculated to

$$C_{12} = C_{23} = \frac{2}{\eta} \quad C_{13} = \frac{4}{\eta^2 + (\Delta - 2)\eta}. \quad (28)$$

In the limit  $\Delta \rightarrow \infty$  the concurrences are vanishing, the states have product form. For the special case  $\Delta = 1$ ,  $|\psi_7\rangle$  and  $|\psi_8\rangle$  have the form of the W-state

$$|\psi_7\rangle = \frac{1}{\sqrt{3}}(|011\rangle + |101\rangle + |110\rangle) = |\widetilde{W}\rangle$$

$$|\psi_8\rangle = \frac{1}{\sqrt{3}}(|001\rangle + |010\rangle + |100\rangle) = |W\rangle$$

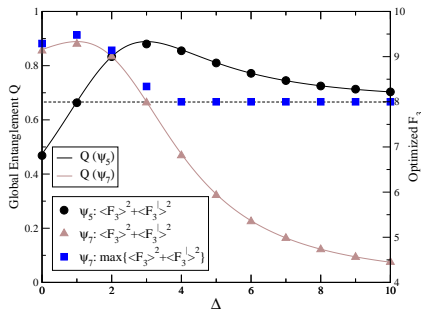


FIG. 2: Comparison of global entanglement  $Q$  and the results of the  $F_3$  optimization for the states  $|\psi_5\rangle$  and  $|\psi_7\rangle$ ; additionally the optimization of  $\langle F_3 \rangle^2 + \langle F'_3 \rangle^2$  for the state  $|\psi_7\rangle$  is plotted.

and the three concurrences are identical. The sum of the squared concurrences is needed for further calculations

$$\sum C_{ij}^2 = 8 \left( \frac{1}{\eta^2} + \frac{2}{(\eta^2 + (\Delta - 2)\eta)^2} \right) \quad (29)$$

From the i-concurrences

$$IC_{1-23} = IC_{3-12} = \frac{1}{\sqrt{2}} \sqrt{1 + \frac{4}{\eta^2} + \frac{2 - \Delta}{\eta}} \quad (30)$$

$$IC_{2-13} = \frac{2\sqrt{2}}{\eta} \quad (31)$$

follows with (12) that  $\tau_{123} = 0$ . Again there is no genuine 3-qubit entanglement as the  $\tau$ -measure indicates. In addition the  $Q$ -measure is calculated (shown in fig. 2). Again, the global entanglement  $Q$  is only a function of the sum of the squared concurrences, which follows directly from equation (16).

In the next section we compare these results with the optimized inequalities.

### C. Comparison with Bell optimization

In fig. 2 besides the global entanglement  $Q$  we plot the results of the Bell optimization as a function of the anisotropy parameter  $\Delta$ . The left y-axis shows  $Q$ , the right one the results for the squared inequalities. For both pairs of states  $|\psi_5\rangle, |\psi_6\rangle$  and  $|\psi_7\rangle, |\psi_8\rangle$  the inequality (3) is violated. This is a sufficient condition for entanglement. With the squared inequalities (4) and (5) we can distinguish 2-qubit and 3-qubit entanglement. The states  $|\psi_5\rangle$  and  $|\psi_6\rangle$  are for  $\Delta > 1.03$  3-qubit entangled. The states  $|\psi_7\rangle$  and  $|\psi_8\rangle$  show 3-qubit entanglement in the range  $0 \leq \Delta \leq 2.97$ . The points that mark the transition between 2-qubit and 3-qubit entanglement were determined by  $\langle F_3 \rangle_\rho^2 + \langle F'_3 \rangle_\rho^2 = 8.01$ .

These results are in accordance with the 3-qubit classification after Dür et al. [10]. There is the so-called W-class of states which are 3-qubit entangled and the tangle is 0. But if we compare the course of the optimized  $F_3$  with

the course of the global entanglement  $Q$  we find - up to an scaling factor - exact analogy. This indicates that an apparent 3-qubit entanglement is due to the fact that the sum of the squared concurrences is larger than 1, the global entanglement  $Q$  larger than  $2/3$ , cp. (16). In the discussion of these parameter dependent states an interesting result is that although both states have no finite tangle they differ in the aspect of the strength of the 2-qubit entanglement as measured by the sum of the squares of the concurrence. As soon as this sum is larger than 1 then there seems to be a kind of effective 3-qubit entanglement which is measured by the optimized  $F_3$  operator. This means, that besides the pure 3-qubit tangle one has to consider the “strength” of the 2-qubit total concurrence, which might effectively describe some indirect 3-qubit entanglement. (But not a genuine one as measured by the tangle.) This means in our interpretation that 3-qubit states with tangle equals to 0 are only 2-qubit entangled.

With our results we conclude that also the W-state is only 2-qubit entangled, because the sum of the squared concurrences is equal to  $4/9$ , cp. [10].

In fig. 2 we plotted additionally the optimization of the squared inequalities for the state  $|\psi_7\rangle$ . For  $\Delta \geq 4$  the optimization yields  $\max\{\langle F_3 \rangle^2 + \langle F'_3 \rangle^2\} = 8.00$  indicating 2-qubit entanglement. As one can see, this method yields the same sufficient conditions to entanglement classification, but less information due to entanglement measurement.

In the following we will discuss the superposition of two states in order to create a state with a finite tangle and to find at the same time the optimized  $F_3$  operator.

### D. Superposition of $|\psi_7\rangle$ and $|\psi_8\rangle$

In this part we will discuss the superposition of the degenerated states  $|\psi_7\rangle$  and  $|\psi_8\rangle$ :

$$\frac{1}{\sqrt{2}} (|\psi_7\rangle + |\psi_8\rangle)$$

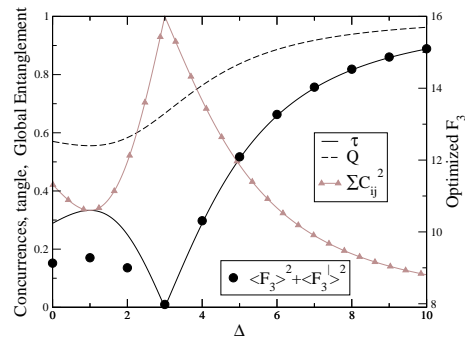


FIG. 3: Measurement of the superposition of  $|\psi_7\rangle$  and  $|\psi_8\rangle$ ; left y-axis: global entanglement, sum of squared concurrences and tangle; right y-axis: optimized  $F_3$  operator.

In the limit  $\Delta \rightarrow \infty$  we get a highly entangled state

$$\frac{1}{\sqrt{2}}(|\psi_7\rangle + |\psi_8\rangle) \approx \frac{1}{\sqrt{2}}(|010\rangle + |101\rangle) \quad (32)$$

The concurrences, the i-concurrences and the tangle can be calculated exactly. The expressions for the concurrence and the tangle are quite long and because of simplicity we will discuss them only graphically.

The calculation of  $Q$  gives the following result:

$$Q = \frac{12 + 5\eta^2 + (\Delta - 2)\eta}{6\eta^2} \quad (33)$$

In fig. 3 we have plotted the sum of the squared concurrences, the global entanglement  $Q$  and the tangle  $\tau$  as a function of  $\Delta$  on the left y-axis. The right y-axis shows the results for the optimization of  $F_3$ .

This superposition of two degenerated states has finite tangle and the sum of the squared concurrences is never larger than 1. From fig. 3 it is interesting to note that at least above  $\Delta = 3$  there is a perfect agreement between the tangle and the optimized  $F_3$  operator. Below  $\Delta = 3$  a tendency of the 3-tangle is reproduced. To sum it up it can be said that the  $F_3$  structure shows tangle like results and therefore measures genuine 3-qubit entanglement.

Altogether one should also note that now the global entanglement measure  $Q$  sums up all different kinds of entanglement, the 2-qubit entanglement as measured by the sum of the squared concurrences and the 3-qubit entanglement as measured by the tangle, cp. (16).

It is remarkable in this respect that the  $F_3$  operator in its optimized form has an interesting structure. E.g. for large  $\Delta$  where the state is mainly a GHZ type state, the operator mainly consists of linear combinations of  $\sigma^x$  and  $\sigma^y$ . There is no contribution from the  $\sigma^z$  components, but it is important to note that although the  $\sigma^x$  contributions are small, they are important in the description of the actual entanglement. This is seen by the fact that if one decreases  $\Delta$  the entanglement decreases and this is seen by the fact that now the  $\sigma^x$  contributions get much stronger although the  $\sigma^z$  components still are negligible. Only for smaller  $\Delta$ , namely in the region of  $\Delta = 3$  where the tangle goes to 0, one clearly sees that our optimized operator has now quite large contributions from  $\sigma^z$ . Looking into the calculation of the tangle one can conclude from this that a finite contribution in  $F_3$  coming from the  $\sigma^z$  operators may indicate a small genuine 3-qubit entanglement.

This gives us sufficient confidence to discuss now 4-qubit systems where an explicit measure of 3- and 4-qubit entanglement is not known. And it turns out that the  $F_4$  optimization will yield additional information. In order to compare with the 3-qubit results we use this time a special isotropic system ( $\Delta = 1$ ) and couple the 4<sup>th</sup> spin with a different coupling constant  $J_s$ .

## VI. PURE 4-QUBIT HEISENBERG STATES

The Hamiltonian of our 4-qubit system can be written as

$$H = \frac{J}{4}(\vec{\sigma}_1\vec{\sigma}_2 + \vec{\sigma}_2\vec{\sigma}_3) + \frac{J_s}{4}(\vec{\sigma}_2\vec{\sigma}_4), \quad (34)$$

with the product  $\vec{\sigma}_i\vec{\sigma}_j = \sigma_i^x\sigma_j^x + \sigma_i^y\sigma_j^y + \sigma_i^z\sigma_j^z$ . The coupling  $J_s$  between spin 2 and 4 attaches the 4<sup>th</sup> spin to the 3 qubits interacting homogeneously. One can easily determine the eigenenergies and states of the system. We find out that two states are of special interest and call them  $|\Phi_1\rangle$  and  $|\Phi_2\rangle$ . They are energetically degenerated and belong to a spin triplet. The abbreviations we use in the following parts, are given in table II.

### A. The state $|\Phi_1\rangle$

The state  $|\Phi_1\rangle$  is of generalized W form and written as

$$|\Phi_1\rangle = a_1|1110\rangle + b_1|1011\rangle + c_1|0111\rangle - c_1|1101\rangle. \quad (35)$$

Because of this structure it is clear from equation (18) that the entanglement of this state is completely described by 2-qubit concurrences. These concurrences have been calculated in the following form:

$$C_{12} = C_{23} = \frac{1}{2\sqrt{2}}\sqrt{1 + \frac{8J(J - J_s)}{\delta^2} + \frac{-5J + 2J_s}{\delta}} \quad (36)$$

$$C_{13} = \frac{1}{2\sqrt{2}}\sqrt{1 - \frac{4J^2}{\delta^2} + \frac{-J + 2J_s}{\delta}} \quad (37)$$

$$C_{14} = C_{34} = \frac{3J + 2J_s + \delta}{4\delta} \quad (38)$$

$$C_{24} = \frac{(J - J_s)(3 + \frac{9J - 2J_s}{\delta})}{6J + 2\delta} \quad (39)$$

Their dependences on the parameters  $J$  and  $J_s$  are given in fig. 4a,b. With these results it is easy to sum the squares with the result given by

$$\sum C_{ij}^2 = \frac{1}{4}\left(5 - \frac{12J^2}{\delta^2} + \frac{-J + 2J_s}{\delta}\right). \quad (40)$$

and the calculation of the global entanglement (cp. (18)) yields (see fig. 4c,d)

$$Q = \frac{1}{8}\left(5 - \frac{12J^2}{\delta^2} + \frac{-J + 2J_s}{\delta}\right). \quad (41)$$

TABLE II: Abbreviations for the 4-qubit model

$\delta = \sqrt{9J^2 - 4JJ_s + 4J_s^2}$	$\mu_2 = \frac{1}{\sqrt{3 + \frac{9J - 2J_s}{\delta}}}$
$a_1 = \frac{1}{2\sqrt{2}\mu_2}$	$b_1 = \frac{J_s - J}{\sqrt{2}\mu_2(3J + \delta)}$
$c_1 = \frac{\mu_2(3J + 2J_s + \delta)}{2\sqrt{18J^2 - 8JJ_s + 8J_s^2}}$	$a_2 = \sqrt{4 + \frac{(-J + 2J_s + \delta)^2}{2J^2}}$

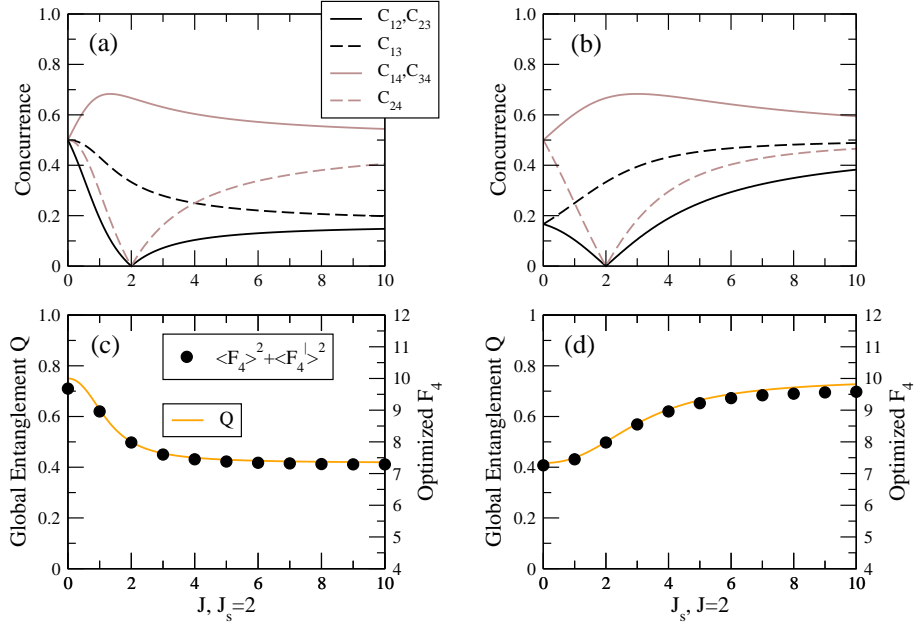


FIG. 4: Concurrences, global entanglement and  $F_4$  optimization for the state  $|\Phi_1\rangle$ ; (a):  $C_{ij}(J, J_s = 2)$ ; (b):  $C_{ij}(J_s, J = 2)$ ; (c): left y-axis:  $Q$ , right y-axis:  $F_4$  optimization, as a function of  $J, J_s = 2$ ; (d): left y-axis:  $Q$ , right y-axis:  $F_4$  optimization, as a function of  $J_s, J = 2$ .

From these figures various conclusions can be drawn. First of all, there are special points in the parameter space where certain concurrences are 0, especially for  $J = J_s = 2$ . From this one can conclude that the qubit 2 can be separated in the state which indeed is true.

$$|\Phi_1\rangle = -\frac{1}{\sqrt{6}}\left(|011\rangle_{134} + |101\rangle_{134} - 2|110\rangle_{134}\right) \otimes |1\rangle_2$$

Furthermore, it can be seen that a total entanglement decreases as a function of  $J$  and increases monotonically as a function of  $J_s$  which means that by coupling these 3 qubits to a 4<sup>th</sup> one in this special state we can increase the total entanglement which can be helpful in certain experimental situations. But most interestingly when we compare these results with the Bell inequality result, we find that the optimized Mermin-Klyshko polynomial operator  $F_4$  is up to a scaling factor the same function as the total global entanglement. But differently from this factor in the case of  $F_4$  one can extract the information that for  $J_s = 2$  and  $J \lesssim 1.94$  as well as for  $J = 2$  and  $J_s \gtrsim 2.06$  the sum of the quadratic concurrences lies above 1 which equals to the fact that we have  $\langle F_4 \rangle^2 + \langle F_4' \rangle^2 > 8$  which indicates an effective 3-qubit entanglement as described above due to the large sum of the squared concurrences. Another interesting aspect can be observed when the interaction constants are 0. When looking at the fig. 4 a,b all the 2-qubit concurrences are unequal to 0 for  $J_s = 2, J = 0$  and  $J = 2, J_s = 0$ . At these values the entanglement is due to symmetry effects and not arising from interaction.

## B. The state $|\Phi_2\rangle$

Even more interesting are the entanglement characteristics for the state  $|\Phi_2\rangle$ . We will apply our reasoning also to this state although one can only give partially quantitative answers. First of all we note that the general form of the state given as

$$|\Phi_2\rangle = -\frac{1}{a_2}|0011\rangle + \frac{1}{a_2}|0110\rangle - \frac{1}{a_2}|1001\rangle + \frac{1}{a_2}|1100\rangle - \frac{J a_2}{2\delta}|0101\rangle + \frac{J a_2}{2\delta}|1010\rangle \quad (42)$$

is quite complicated but it reduces to a GHZ state in the two limits  $J_s = 2$  and  $J \rightarrow 0$  as well as  $J = 2$  and  $J_s \rightarrow \infty$ :

$$|\Phi_2\rangle \rightarrow -\frac{1}{\sqrt{2}}\left(|0101\rangle - |1010\rangle\right). \quad (43)$$

From this we can conclude that there must be besides the 2-qubit concurrences an additional 3- and/or 4-qubit entanglement.

For the concurrences one finds:

$$C_{12} = C_{14} = C_{23} = C_{34} = \max\left\{0, \frac{2J}{\delta} - \frac{4J^2}{8\delta^2 + (2J_s - J + \delta)^2}\right\} \quad (44)$$

$C_{12}, C_{14}, C_{23}$  and  $C_{34}$  are greater or equal than 0 for  $J_s = 2, J > 0$  resp.  $J = 2, J_s > 0$ . The exact analytic representation of  $C_{13}$  and  $C_{24}$  is only possible in

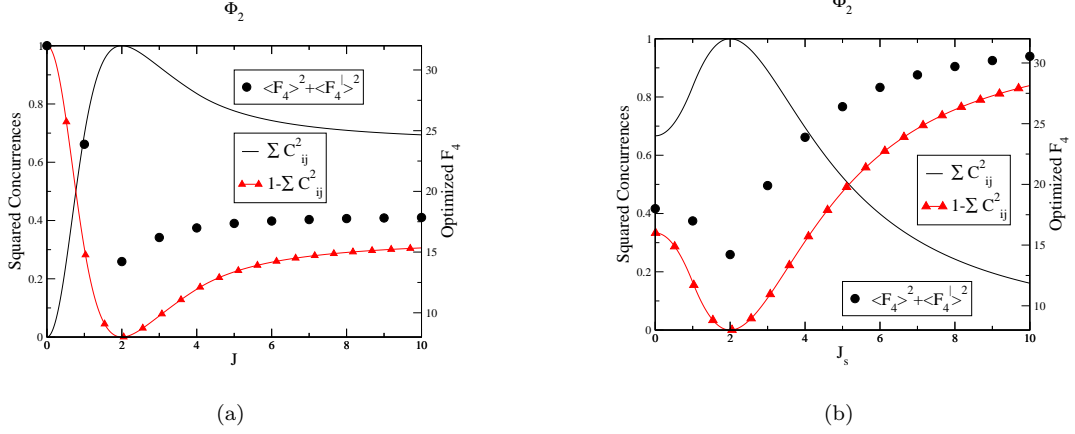


FIG. 5: Comparison of the sum of the squared concurrences and the  $F_4$  optimization for the state  $|\Phi_2\rangle$ .

TABLE III: Parameters out of the  $F_4$  optimization for the state  $|\Phi_2\rangle$ ;

$J_s = 2, J = 0$				$J_s = 0, J = 2$					
A	$\sigma_A^x$	7.33587e-01	$\sigma_{A'}^x$	-6.79595e-01	A	$\sigma_A^x$	7.52415e-01	$\sigma_{A'}^x$	3.37233e-01
	$\sigma_A^y$	6.79595e-01	$\sigma_{A'}^y$	7.33587e-01		$\sigma_A^y$	5.16326e-01	$\sigma_{A'}^y$	2.31417e-01
	$\sigma_A^z$	2.11433e-07	$\sigma_{A'}^z$	2.93477e-07		$\sigma_A^z$	-4.08998e-01	$\sigma_{A'}^z$	9.12535e-01
B	$\sigma_B^x$	6.72877e-01	$\sigma_{B'}^x$	7.39754e-01	B	$\sigma_B^x$	8.07789e-01	$\sigma_{B'}^x$	1.65322e-01
	$\sigma_B^y$	7.39754e-01	$\sigma_{B'}^y$	-6.72877e-01		$\sigma_B^y$	5.54324e-01	$\sigma_{B'}^y$	1.13448e-01
	$\sigma_B^z$	1.93281e-07	$\sigma_{B'}^z$	2.55498e-07		$\sigma_B^z$	-2.00504e-01	$\sigma_{B'}^z$	9.79693e-01
C	$\sigma_C^x$	6.28202e-01	$\sigma_{C'}^x$	7.78050e-01	C	$\sigma_C^x$	7.43104e-01	$\sigma_{C'}^x$	3.57282e-01
	$\sigma_C^y$	-7.78050e-01	$\sigma_{C'}^y$	6.28202e-01		$\sigma_C^y$	5.09936e-01	$\sigma_{C'}^y$	2.45176e-01
	$\sigma_C^z$	-1.48041e-07	$\sigma_{C'}^z$	-1.92036e-07		$\sigma_C^z$	-4.33315e-01	$\sigma_{C'}^z$	9.01242e-01
D	$\sigma_D^x$	1.90480e-01	$\sigma_{D'}^x$	9.81691e-01	D	$\sigma_D^x$	2.32613e-01	$\sigma_{D'}^x$	7.91041e-01
	$\sigma_D^y$	9.81691e-01	$\sigma_{D'}^y$	-1.90481e-01		$\sigma_D^y$	1.59625e-01	$\sigma_{D'}^y$	5.42831e-01
	$\sigma_D^z$	-1.79827e-07	$\sigma_{D'}^z$	3.21086e-07		$\sigma_D^z$	9.59381e-01	$\sigma_{D'}^z$	-2.82115e-01

the parameter ranges  $J = 2, J_s < 2$  and  $J_s = 2, J > 2$ :

$$C_{13} = C_{24} = \max\left\{0, \frac{1}{\sqrt{2}\delta} \left( \sqrt{\delta^2 + \delta(J - 2J_s) - 4J^2} - \sqrt{\delta^2 - \delta(J - 2J_s) - 4J^2} \right)\right\} \quad (45)$$

For  $J = 2, J_s \geq 1$  and  $J_s = 2, J \leq 4$ ,  $C_{13}$  and  $C_{24}$  are equal to 0.

In fig. 5 we have plotted the sum of the squares of the concurrences. We can see that the maximum is at  $J_s = J = 2$ . It drops for very large  $J_s$  to 0 while for  $J$  to infinity it levels to a finite value. Furthermore, it is found that the total global entanglement is constantly 1

$$Q(|\Phi_2\rangle) = 1, \quad (46)$$

which means that there is no differentiation between the different qubit entanglements in this measure. Again it is very remarkable that the Mermin-Klyshko optimized

operator is describing the additional entanglement (besides the 2-qubit concurrences) and follows parallel to the curve  $1 - \sum C_{ij}^2$ . We therefore conclude in analogy to the 3-qubit case that  $F_4$  measures the true 3- and 4-qubit entanglements for this state. This is the most interesting result of our paper, since here is a quantitative measure of  $n$ -qubit entanglement ( $n = 3, 4$ ) for a 4-qubit state, although we cannot discriminate between 3- and 4-qubit entanglement.

Again if we look for the structure of  $F_4$  we find that all polynomial contributions for the limits  $J_s = 2, J = 0$  and  $J = 2, J_s \rightarrow \infty$  come from products of  $\sigma^x$  and  $\sigma^y$  for the different qubits and that the weight of this contribution changes with the strength of the additional entanglement (cp. Table III).

In a future paper the polynomial structure is investigated in detail.



## VII. CONCLUSIONS AND DISCUSSIONS

It is shown in this paper that the optimized Mermin-Klyshko operators can be used very effectively to describe the degree of entanglement in different clusters of Heisenberg spins. In those cases where there is in the 3-qubit system besides the concurrences no additional entanglement (i. e. the tangle  $\tau = 0$ ) the optimized  $F_3$  operator perfectly describes the 2-qubit entanglement of the system as a function of the anisotropic parameter in the Heisenberg cluster and it is more or less identical to the global entanglement measure resp. the sum of the squared concurrences, cp. (16). In those cases where in addition to the 2-qubit concurrences there is a finite tangle  $\tau$ , we find that this additional 3-qubit entanglement measured by  $\tau$  is nearly perfect described by the optimized  $F_3$ , as shown in fig. 3.

We therefore test this result in a 4-qubit system and again we find two different cases. We discuss a special state  $|\Phi_1\rangle$  where the sum of the 2-qubit concurrences is mainly proportional to the global entanglement measure and from this we find that the optimized  $F_4$  operator follows this  $Q$  value. In the second eigenstate for the

system  $|\Phi_2\rangle$  where the global entanglement is just equal to 1, independent of the parameters, we expect besides the 2-qubit concurrences an additional entanglement and this seems to be perfectly the case, especially when the expression  $1 - \sum C_{ij}^2$  is compared in its parameter dependence to the optimized  $F_4$ , shown in fig. 5. Our special interest is here that even at the minima of these functions, at the point  $J = J_s = 2$ , there is a small but finite higher entanglement which of course at the moment could not be interpreted as 3- or otherwise 4-qubit entanglement.

It should be noted that the optimization procedure for the  $F_N$  operators heavily depends on the starting values and therefore a procedure has to be used where a random choice for the starting values has to be done. Another remark is, that this optimization yields much more than one minimum or maximum and therefore one should be careful with the interpretation of these parameters. But at least for the GHZ-state with 4-qubits we have shown that these operators contain besides the usually used  $\sigma^y$  operators additional  $\sigma^x$  contributions [18].

Further work is in preparation where a more extensive study of these  $F_N$  operators will be presented.

- 
- [1] A.K. Ekert, Phys. Rev. Lett. **67**, 661 (1991).
  - [2] C.H. Bennett and S.J. Wiesner, Phys. Rev. Lett. **69**, 2881 (1992).
  - [3] C.H. Bennett *et al.*, Phys. Rev. Lett. **70**, 1895 (1993).
  - [4] D. Meyer and N. Wallach, J. Math. Phys. **43**, 4273 (2002), quant-ph/0108104.
  - [5] N.D. Mermin, Phys. Rev. Lett. **65**, 1838 (1990).
  - [6] D. Klyshko, Phys. Lett. A **172**, 399 (1993).
  - [7] A. Belinskii and D. Klyshko, Physics - Uspekhi **36**, 653 (1993).
  - [8] S. Yu, Z.B. Chen, J.W. Pan, and Y.D. Zhang, Phys. Rev. Lett. **90**, 080401 (2003), quant-ph/0211063.
  - [9] D. Greenberger, M. Horne, and A. Zeilinger, Going beyond bell's theorem, in *Bell's Theorem, Quantum Theory and Conceptions of the Universe*, edited by M. Kafatos, p. 69, Kluwer Academic Publishers, 1989.
  - [10] W. Dür, G. Vidal, and J.I. Cirac, Phys. Rev. A **62**, 062314 (2000), quant-ph/0005115.
  - [11] G. Brennen, QIC **3**, 619 (2003), quant-ph/0305094.
  - [12] P. Rungta, V. Buzek, C.M. Caves, M. Hillery, and G.J. Milburn, Phys. Rev. A **64**, 042315 (2001), quant-ph/0102040.
  - [13] V. Coffman, J. Kundu, and W.K. Wootters, Phys. Rev. A **61**, 052306 (2000), quant-ph/9907047.
  - [14] S. Hill and W.K. Wootters, Phys. Rev. Lett. **78**, 5022 (1997), quant-ph/9703041.
  - [15] W.K. Wootters, Phys. Rev. Lett. **80**, 2245 (1998), quant-ph/9709029.
  - [16] V. Scarani and N. Gisin, J. Phys. A: Math. Gen. **34**, 6043 (2001), quant-ph/0103068.
  - [17] U. Glaser, H. Büttner, and H. Fehske, Phys. Rev. A **68**, 032318 (2003), quant-ph/0305108.
  - [18] G. Jaeger, A.V. Sergienko, B.E.A. Saleh, and M.C. Teich, Phys. Rev. A **68**, 022318 (2003), quant-ph/0307124.
  - [19] <http://www.nag.co.uk>